EUROPEAN ORGANIZATION FOR NUCLEAR RESEARCH

MESON RESONANCE PRODUCTION IN $\pi^- p \to K^0_S K^- p$ AT 10 GeV/c

R. Baldi, T. Böhringer, P.A. Dorsaz, V. Hungerbühler,
M.N. Kienzle-Focacci, M. Martin, A. Mermoud, C. Nef and P. Siegrist

University of Geneva, Switzerland
and
CERN, Geneva, Switzerland

We have collected 40,000 events on the reaction $\pi^- p \to K^0_S K^- p$ at 10 GeV/c with the Geneva spectrometer at CERN PS during the years 1975-76.

Resonances of the $K^0_S K^-$ system are observed in the invariant mass range 1.0-2.0 (GeV/c) and momentum transfer range $0.07 \leq t \leq 1.0$ $(\text{GeV/c})^2$.

A spherical harmonics moments analysis is made as a function of $(K^0_S K^-)$ mass and as a function of t for the $A_2(1315)$ and g(1700) resonances. From the moment analysis we get evidence for the presence of an $I = 1$, $J^P = 4^+$, object near 1950 MeV.

Presented at the
European Conference on Particle Physics
Budapest, Hungary, 4-9 July 1977

Geneva - 23 June 1977

INTRODUCTION

The two-arm spectrometer of the Geneva University was mainly designed for K^* studies in an unseparated K beam at 10 GeV/c at the CERN Proton Synchrotron (PS). Owing to its high acquisition capability, this system simultaneously recorded π^--induced reactions from which we have analysed 40,000 $\pi^- p \to K^0_S K^- p$ events.

The spectrometer, data acquisition, and event reconstruction are described elsewhere[1] for the channel $K^\pm p \to K^0_S \pi^\pm p$. Here we study the $K^0_S K^-$ system and present moments of the angular distributions versus $(K^0_S K^-)$ effective mass between 1.0 and 2.0 GeV and versus momentum transfer $|t_{pp}|$ between 0.07 and 1.0 $(GeV/c)^2$.

1. DATA SELECTION

We recorded 7.5×10^7 π incident triggers with at least three tracks in the forward spectrometer. This topological requirement was achieved by a hardware logic on the MWPC planes, eliminating all elastic events and also inelastic events outside the forward system acceptance. A reconstruction program checking the π incident track, the p recoil track, and the $p\pi$ vertex parameters reduced the set of candidate events to about 3×10^7.

Channel selection was then applied in two steps:

i) a geometrical search of a second vertex at least 30 mm downstream from the $p\pi$ vertex in order to discriminate between the $K^0_S K^- (K^0_S \to \pi^+\pi^-)$ and the $\pi^- p \to \pi^+\pi^-\pi^- p$ channel;

ii) a kinematical fit on the measured quantities (track parameters, incident and recoil proton momenta), with five equations (energy-momentum conservation at the production vertex and at the K^0_S decay vertex) and three unknowns (three moduli of the forward momenta), gave us a 2C fit. The number of fitted events with $P(\chi^2) > 5\%$ was then about 40,000 with an estimated background of 6% under the K^0 mass. An additional cut was made on pK^- effective masses smaller than 1.9 GeV to eliminate the main Y^* contributions and their kinematical reflections at high $K^0_S K^-$ masses.

2. MOMENT ANALYSIS OF THE A_2 AND g RESONANCES

2.1 The $(K^0_S K)$ mass spectrum between 1.0 and 1.8 GeV

The acceptance-corrected spherical harmonics moments $\sqrt{4\pi}\ N\ \mathrm{Re}\ \langle Y^M_L \rangle$ of the K^- angular distribution were calculated in the t-channel helicity frame of the $(K^0_S K^-)$ system (the Y^M_L normalization used is $\int Y^M_L Y^{M'}_{L'} d\Omega = 4\pi$). In Figs. 1a and 1b the unnormalized moments are displayed versus $M(K^0_S K^-)$ in 50 MeV bins from 1.0 to 2.0 GeV and integrated over $|t|$ from 0.07 to 1.0 $(GeV/c)^2$. It was assumed that

the only moments significantly different from zero were those with $0 \leq L \leq 8$, $0 \leq M \leq 2$. These 24 corrected moments were obtained from the overdetermined linear system of 66 equations for the 66 uncorrected moments with $0 \leq L \leq 10$, $0 \leq M \leq L$ (Ref. 1). The $\langle Y_0^0 \rangle$ and other higher-order moments show clear A_2 and g signals. A least squares fit on the $\langle Y_0^0 \rangle$ with two Breit-Wigner functions gave $M_{A_2} = 1315 \pm \pm 0.5$, $\Gamma_{A_2} = 103 \pm 2$ MeV and $M_g = 1707 \pm 7$, $\Gamma_g = 152 \pm 14$ MeV (statistical errors from the fit only).

We can express the moments in terms of amplitudes:

$$\left\langle Y_{2J}^0 \right\rangle \sim C_1 \left|M_0^J\right|^2 - C_2 \left(\left|M_-^J\right|^2 + \left|M_+^J\right|^2 \right)$$

$$\left\langle Y_{2J}^0 \right\rangle \sim C_3 \left(\left|M_-^J\right|^2 - \left|M_+^J\right|^2 \right) .$$

where M_0^J is the spin-J helicity zero amplitude produced by unnatural parity exchange (UPE) in the t-channel; $M_\pm^J$ are the spin-J helicity 1 amplitudes produced by NPE and UPE (Ref. 1); $C_1C_2C_3$ are positive coefficients (Clebsch-Gordan). Contributions from waves with lower J are neglected. The spin-2 A_2 resonance exhibits strong negative $\langle Y_4^0 \rangle$ and $\langle Y_4^2 \rangle$ moments, while the spin-3 g has a positive signal in $\langle Y_6^0 \rangle$. This implies that A_2 production seems to be dominated by NPE, D_+-wave (M_+^2), and g production by UPE, mainly F_0-wave (M_0^3). More precisely, in the t-channel at the meson vertex the $\mathbb{P}$, f, ρ exchanges dominate over B exchange for the A_2, while π exchange dominates over ω, ϕ, A_2 exchanges in the g region (G-parity conservation forbids π exchange in the A_2 region). However, the g signal is partly suppressed in our data by the high $|t|$ range acceptance (> 0.07 GeV/c^2), unfavourable to π-exchange production.

In the A_2 mass region a better fit for moments is obtained when adding terms with M = 3 and 4, which suggests that at 10 GeV/c the A_2 is not purely produced in a helicity 1 state. In Fig. 2, moments in 25 MeV bins show this effect, especially $\langle Y_4^3 \rangle$ with a clear signal at the A_2 mass due to interference between helicity 1 and 2 states.

2.2 t-dependence of the A_2 and g mesons

As a consequence of the existence of the L = 3 terms shown above, we have calculated moments up to L = 4, M = 4 versus $|t|$ integrated over the A_2 region $\left[1.2 \leq M(K^0K^-) \leq 1.4 \text{ GeV}\right]$ in the $|t|$ interval $0.07 \leq |t| \leq 0.81$ (GeV/c)^2 shown in Fig. 3. The NPE contribution to A_2 production is clearly seen from the sign and intensity of $\langle Y_4^0 \rangle$ and $\langle Y_4^2 \rangle$ moments as discussed in the previous section. An expression of the type $N(t) \sim t' e^{-bt'}$, with $t' = |t - t_{min}|$, was fitted to $\langle Y_0^0 \rangle$, $\langle Y_4^0 \rangle$ and $\langle Y_4^2 \rangle$ in the $|t|$ interval 0.09-0.61 (GeV/c)^2, and gave respectively the values $b(Y_0^0) = 8.00 \pm 0.06$ (GeV/c)$^{-2}$; $b(Y_4^0) = 7.99 \pm 0.12$ (GeV/c)$^{-2}$; $b(Y_4^2) = 7.88 \pm 0.10$ (GeV/c)$^{-2}$ with good probabilities of χ^2.

Figures 4a and 4b display moments versus t up to L = 6, M = 2 integrated over $M(K^0K)$ from 1.55 to 1.85 GeV, between 0.07 and 0.79 $(GeV/c)^2$. The positive $\langle Y_6^0 \rangle$ drops rapidly with increasing $|t|$ as expected for π exchange, and reaches zero near $|t| \simeq 0.35$ $(GeV/c)^2$.

3. THE HIGH $K_S^0K^-$ MASSES

In Figs. 1a and 1b most of the moments seem to indicate some structure in the mass region greater than 1.8 GeV where we may expect some new spin state. Especially the L = 7 moments characteristic of interference between F- and G-waves, and the L = 8 moments indicative of a spin-4 object, have significantly non-zero values.

As the mass range depends on $|t|$, we have removed events with $0.07 \leq |t| \leq 0.15$ $(GeV/c)^2$ in order to eliminate events with too small acceptance. We have then fitted the angular distribution from 1.4 to 2.125 GeV in 50 MeV bins integrated over the $|t|$ interval 0.15-1.0 $(GeV/c)^2$ by the extended maximum likelihood method[2] with a set of 24 unnormalized moments $\langle Y_L^M \rangle$ $0 \leq L \leq 8$, $0 \leq M \leq 2$ as shown in Figs. 5a and 5b. Results are consistent with the previous fit. Non-zero L = 7 (4 st. dev.) and L = 8 (5 st. dev.) moments show evidence for a G-wave with I = 1, positive parity, starting near 1800 MeV with a maximum around 1950 MeV. We may estimate a width of about 150 MeV, but a more accurate determination of mass and width will need a better high mass acceptance [comparison can be made with the I = 0 G-wave resonance in $\pi^- p \to K^+K^- n$ [3]]. The negative signs of the moments $\langle Y_8^0 \rangle$, $\langle Y_8^2 \rangle$ indicate that this spin-4 wave seems to be mainly produced via NPE, and the absence of π exchange suggests negative G-parity.

4. CONCLUSIONS

The good statistics and low background sample obtained in this experiment gives information on A_2 and g parameters and production mechanisms. The fitted slope of the A_2 $d\sigma/dt$ compared with values at higher energies[4,5] seems to indicate a constant behaviour with increasing energy. The g meson is shown to be produced mainly by UPE at small $|t|$ values. Finally, a significant I = 1 positive parity G-wave is obtained near 1950 MeV.

REFERENCES

1) R. Baldi et al., Systematic study of $K\pi$ production in the reaction $K^{\pm}p \rightarrow$ $\rightarrow K^0_S\pi^{\pm}p$: Techniques and measurements at 10 GeV/c, submitted to the EPS Conference, Budapest (1977).

2) J. Orear, Notes on statistics for physicists, UCRL 8417 (1958).

3) W. Blum et al., Evidence for a spin-4 boson resonance at 2050 MeV, submitted to the EPS International Conference on High-Energy Physics, Palermo, June, 1975.

4) R. Klanner, Analysis of the reaction $\pi^-p \rightarrow \pi^-\pi^-\pi^+p$ at 25 and 40 GeV/c. Thesis, Munich University, 1973.

5) M. Margulies et al., High statistics investigations of K^0K^- decays of A_2^- produced by 23 GeV/c π^- on hydrogen, BNL-21353.

Figure captions

Fig. 1a and 1b : Unnormalized corrected spherical harmonics moments of angular distribution of the K^- in the t-channel helicity rest frame of the $K^0_S K^-$ system at 10 GeV/c: $\sqrt{4\pi}\ N\ \langle Y^M_L \rangle$, $M(K^0_S K^-)$ 1.0-2.0 GeV, 50 MeV bins, $0.07 \leq |t| \leq 1.0$ $(GeV/c)^2$, L = 0 to 8 with M = 0, 1, 2.

Fig. 2 : Part of $\sqrt{4\pi}\ N\ \langle Y^M_L \rangle$ for $M(K^0K^-)$ 1.0 to 1.6 GeV, $0.07 \leq |t| \leq$ ≤ 1.0 $(GeV/c)^2$, L = 0 to 6, M = 0 to 4, showing evidence for helicity 2 A_2 production.

Fig. 3 : $\sqrt{4\pi}\ N\ \langle Y^M_L \rangle$ as function of $|t|$ in A_2 mass region: $1.2 \leq M(K^0_S K^-) \leq$ ≤ 1.4 GeV, $0.07 \leq |t| \leq 0.81$ $(GeV/c)^2$, L = 0 to 4, M = 0 to 4.

Fig. 4a and 4b : $\sqrt{4\pi}\ N\ \langle Y^M_L \rangle$ as function of $|t|$ in g-mass region: $1.55 \leq M(K^0_S K^-) \leq$ ≤ 1.85 GeV, $0.07 \leq |t| \leq 0.79$ $(GeV/c)^2$, L = 0 to 6, M = 0 to 2.

Fig. 5a and 5b : $\sqrt{4\pi}\ N\ \langle Y^M_L \rangle$ as function of $M(K^0_S K^-)$: $1.4 \leq M(K^0_S K^-) \leq 2.125$ GeV, $0.15 \leq |t| \leq 1.0$ $(GeV/c)^2$, L = 0 to 8, M = 0 to 2. Likelihood fit.

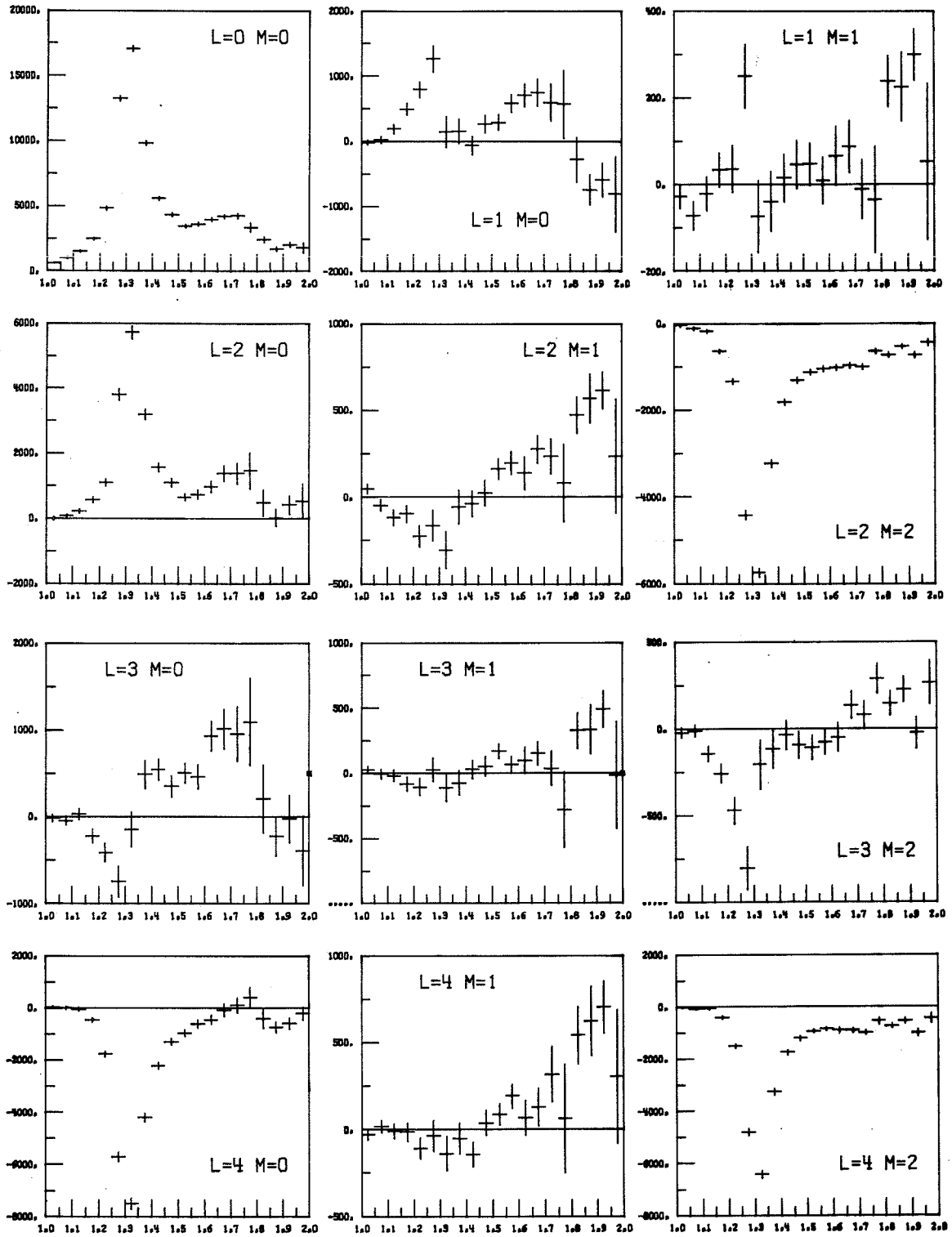

Fig. 1 a)

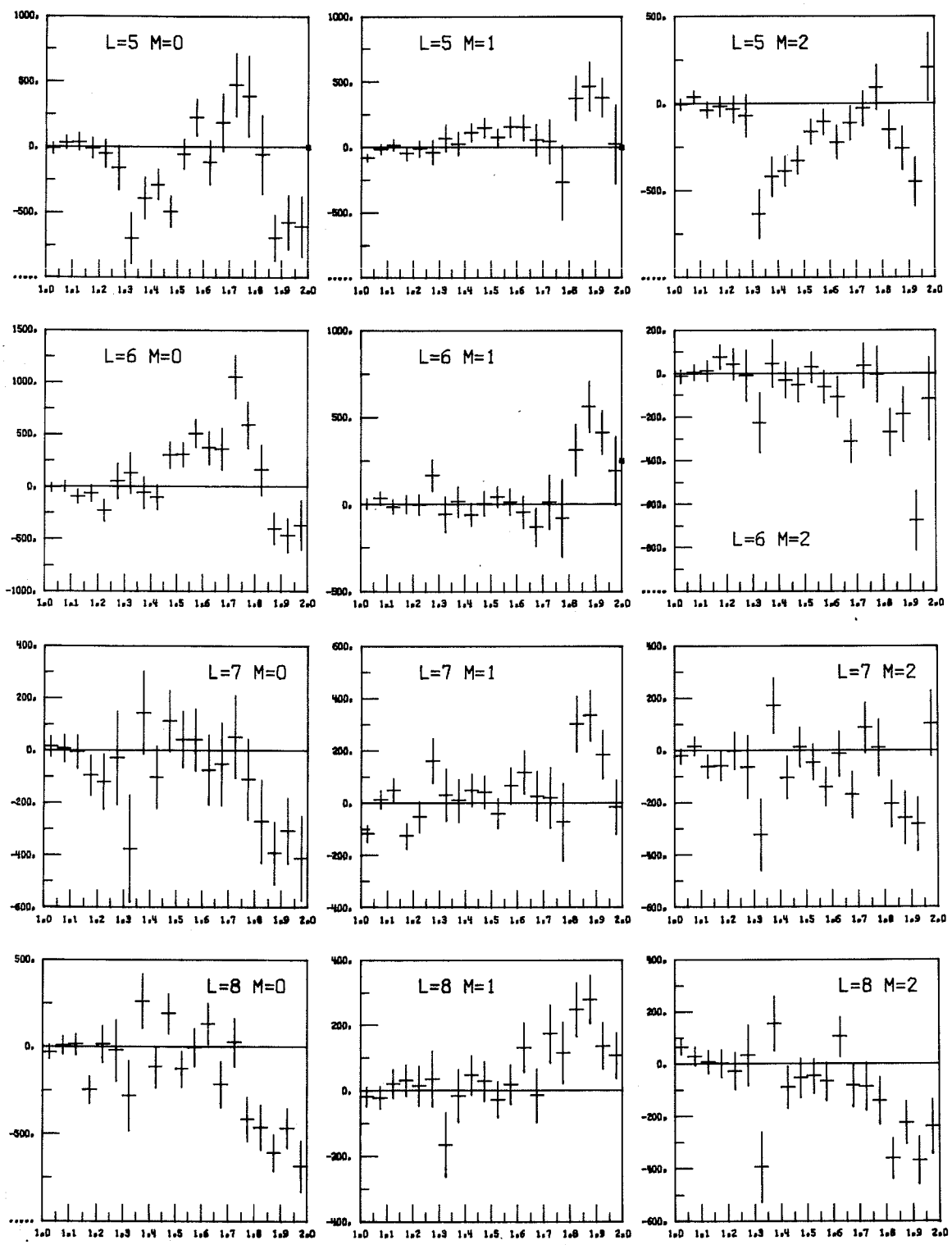

Fig. 1 b)

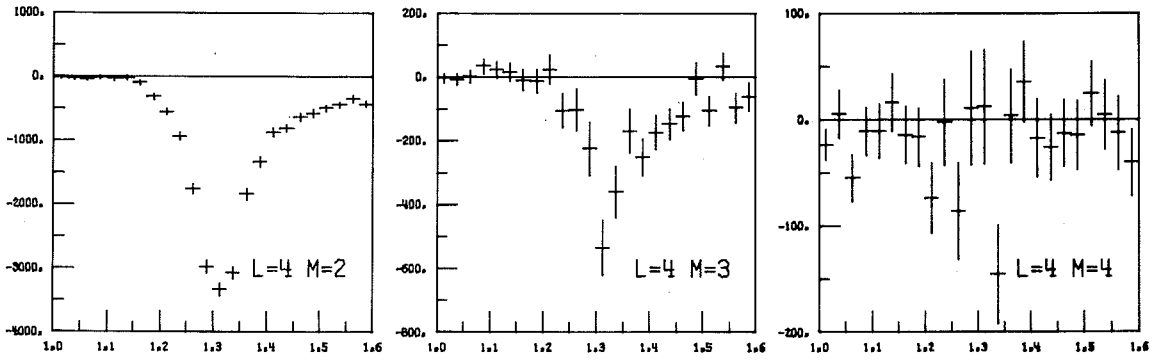
1000.
0.
-1000.
-2000.
-3000.
-4000.
1.0
1.1
1.2
1.3
1.4
1.5
1.6
L=4 M=2
200.
0.
-200.
-400.
-600.
-800.
L=4 M=3
100.
0.
-100.
-200.
L=4 M=4

Fig. 2

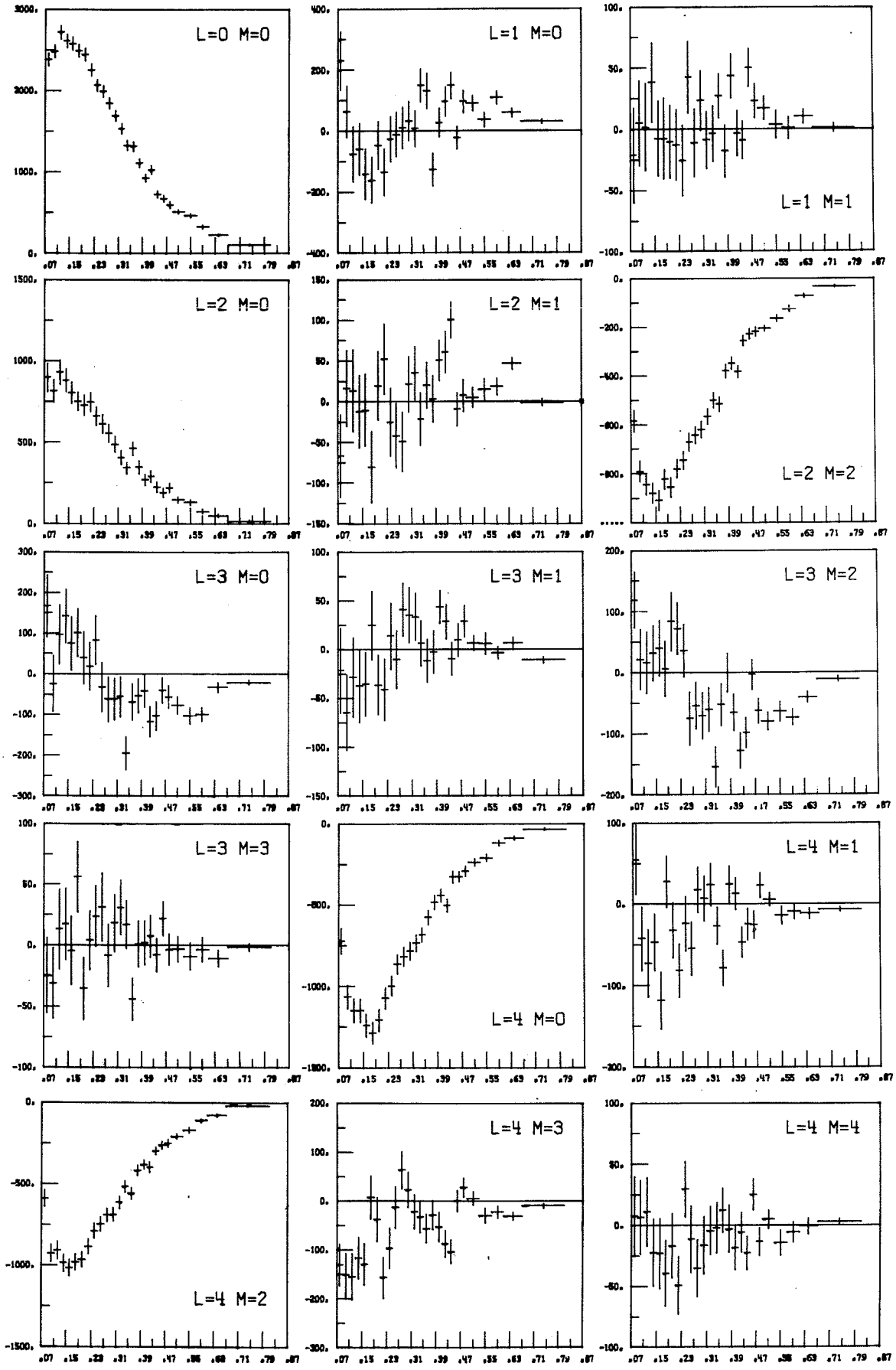
L=0 M=0
L=1 M=0
L=1 M=1
L=2 M=0
L=2 M=1
L=2 M=2
L=3 M=0
L=3 M=1
L=3 M=2
L=3 M=3
L=4 M=0
L=4 M=1
L=4 M=2
L=4 M=3
L=4 M=4

Fig. 3

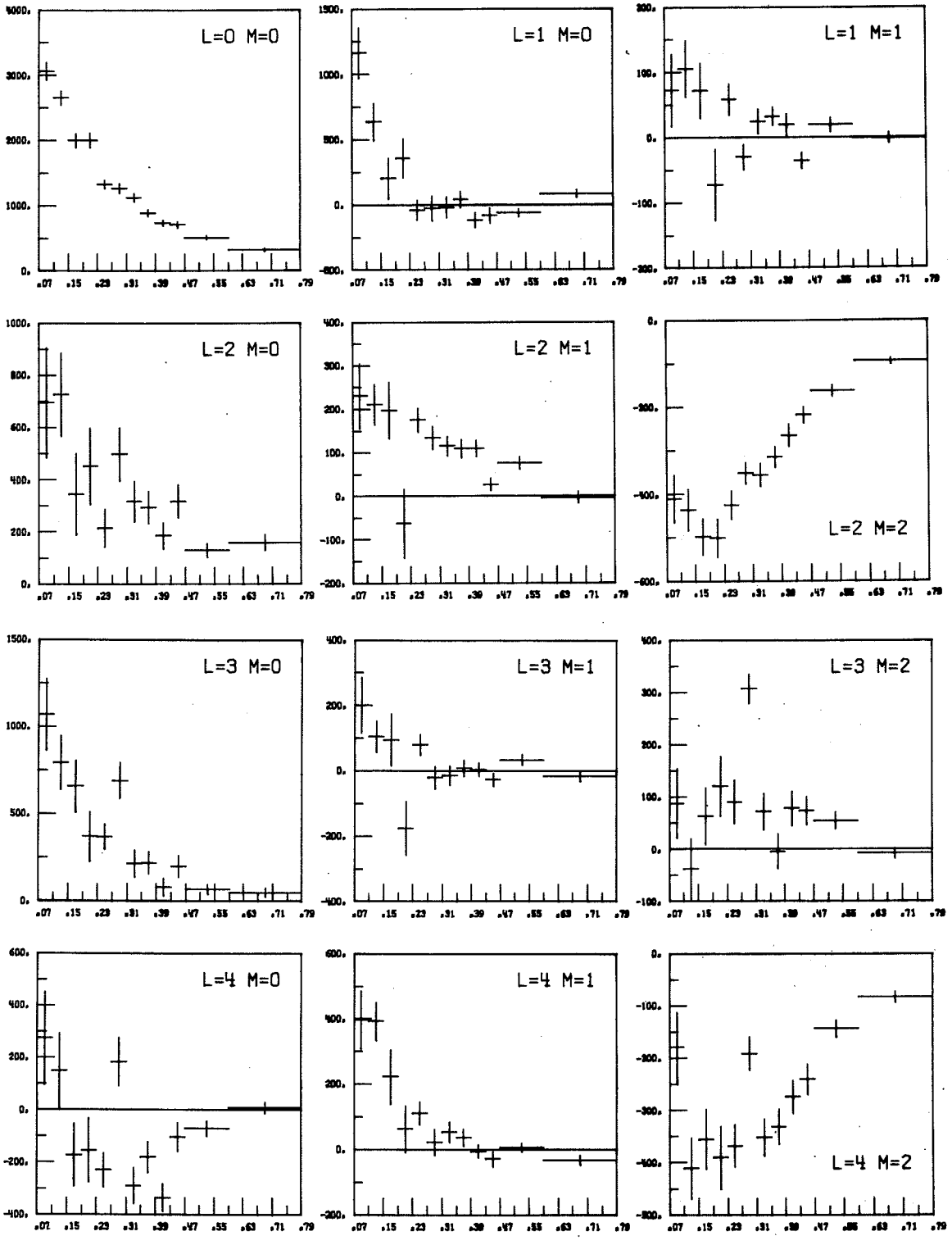

Fig. 4 a)

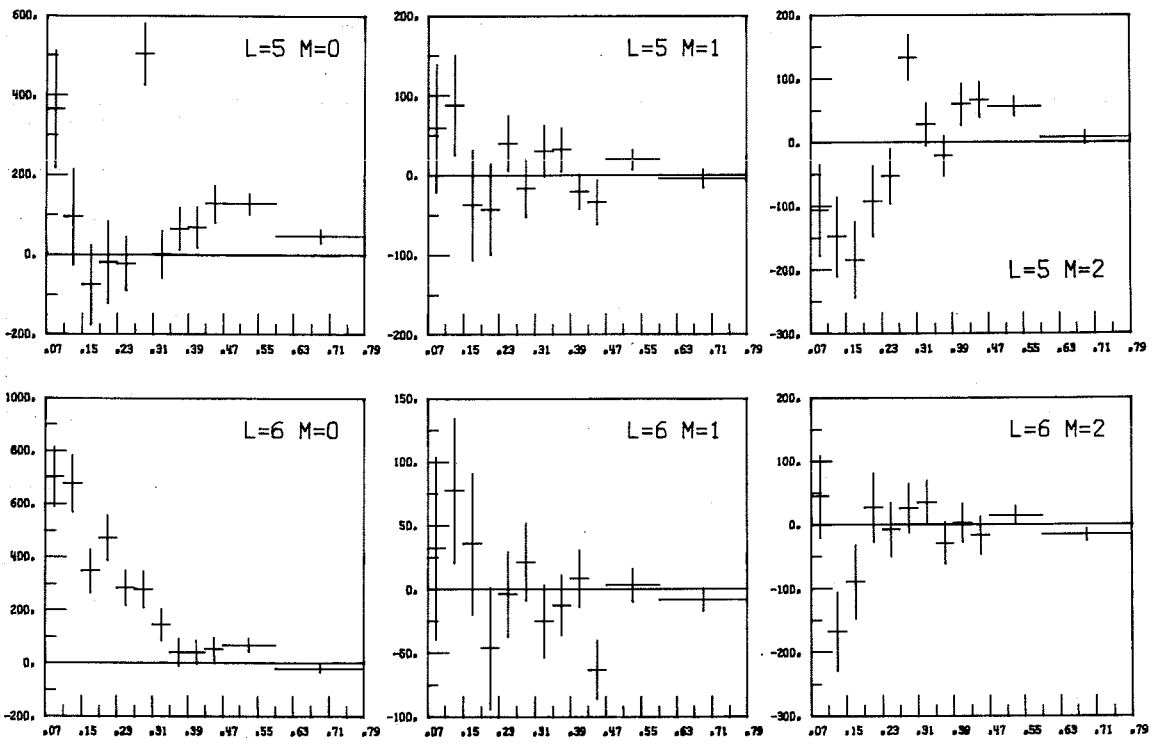

Fig. 4 b)

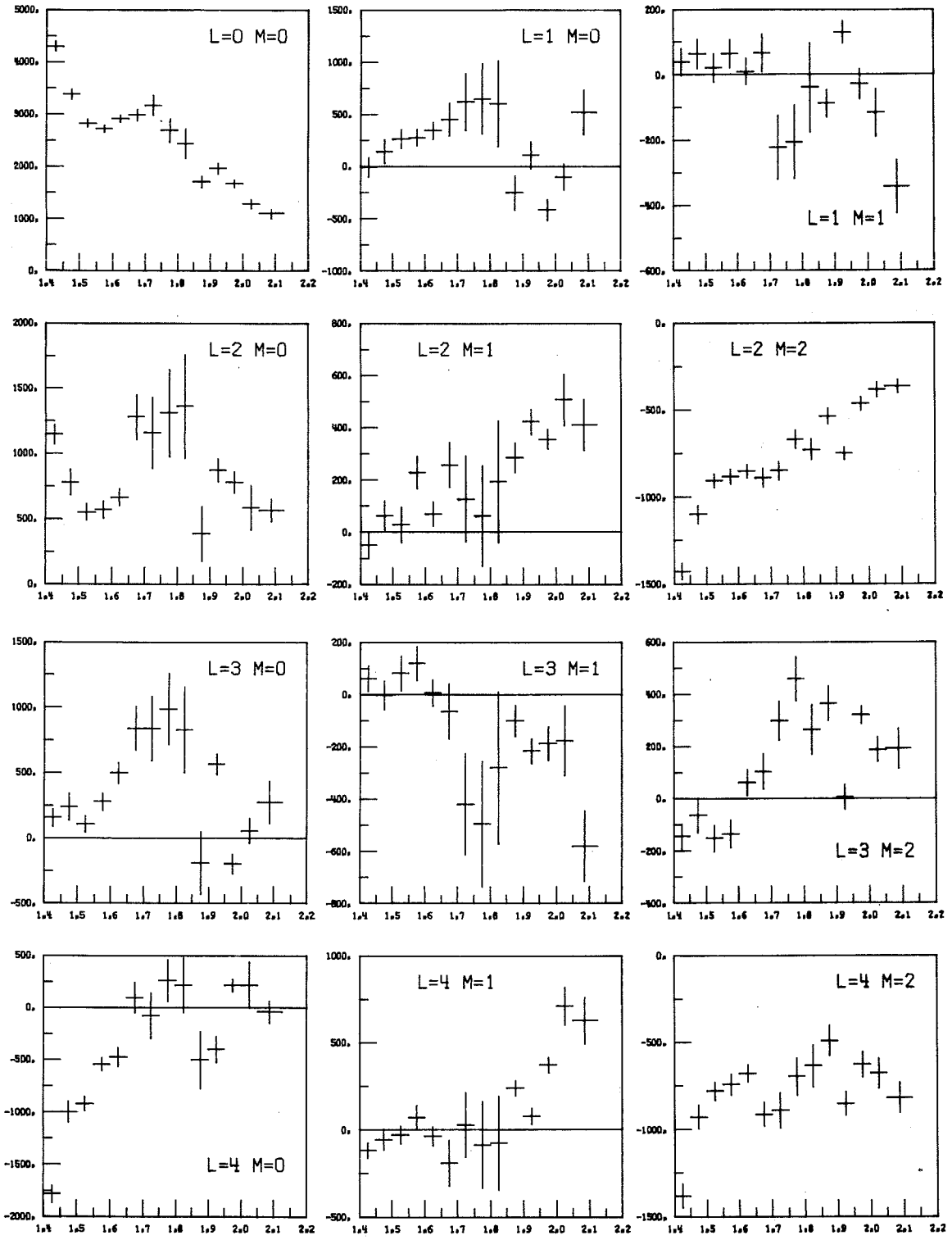

Fig. 5 a)

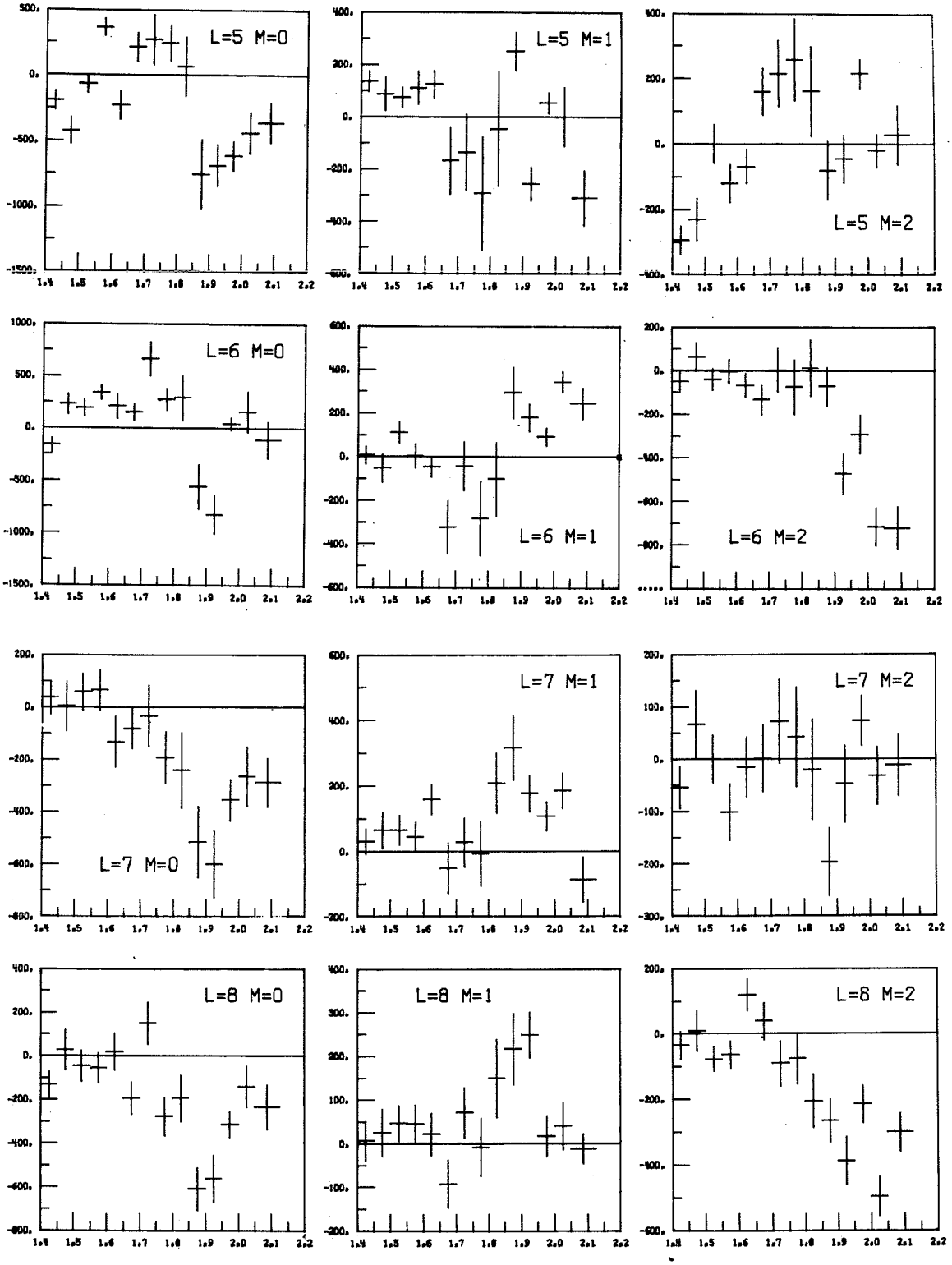

Fig. 5 b)